minerals

Article

Thermally Assisted Grinding of Cassiterite Associated with Pollimetallic Ore: A Comparison between Microwave and Conventional Furnaces

Chunlin He [1,2,*], Jian Zhao [1,2], Xiujuan Su [1,*], Shaojian Ma [1,2], Toyohisa Fujita [1,2], Yuezhou Wei [1,2,3], Jinlin Yang [1,2] and Zongwu Wei [1,2]

1 School of Resources, Environment and Materials, Guangxi University, Nanning 530004, China; ZJ19780823@163.com (J.Z.); msj@gxu.edu.cn (S.M.); fujitatoyohisa@gxu.edu.cn (T.F.); yzwei@gxu.edu.cn (Y.W.); 1615391004@st.gxu.edu.cn (J.Y.); fangshen@gxu.edu.cn (Z.W.)
2 Guangxi Key Laboratory of Processing for Non-Ferrous Metal and Featured Materials, Nanning 530004, China
3 School of Nuclear Science and Engineering, Shanghai Jiao Tong University, Shanghai 200240, China
* Correspondence: helink@gxu.edu.cn (C.H.); zhsxty@gxu.edu.cn (X.S.)

Abstract: We investigated the influence of microwave and conventional heating pretreatments on the grinding of cassiterite associated with pollimetallic ore. The minerals that exhibited a stronger microwave absorption ability crushed first, which is the main difference between the microwave and the traditional heating pretreatments. The distribution of Fe, Pb, Zn, and Sn increased in the fine size range (−0.425 mm). The Fe and Pb grades in the size ranges of −3.2 + 2 mm and −2 + 1 mm after the microwave pretreatment (6 kW, 1 min) were lower than those of the traditional heating (12 kW, 400 °C, 20 min), indicating that the microwave selective heating was beneficial for pyrite and jamesonite. The grade and distribution of Sn decreased significantly in the size ranges of −3.2 + 2 mm and −2 + 1 mm and increased in the size ranges of −0.425 + 0.15 mm and −0.15 + 0.074 mm. Microwave heating treatment promoted the grinding of sulfide ore and reduced the cassiterite overgrinding.

Keywords: cassiterite; microwave heating; sulfide ore; grinding

Citation: He, C.; Zhao, J.; Su, X.; Ma, S.; Fujita, T.; Wei, Y.; Yang, J.; Wei, Z. Thermally Assisted Grinding of Cassiterite Associated with Pollimetallic Ore: A Comparison between Microwave and Conventional Furnaces. *Minerals* **2021**, *11*, 768. https://doi.org/10.3390/min11070768

Academic Editor: Pura Alfonso

Received: 14 June 2021
Accepted: 13 July 2021
Published: 15 July 2021

1. Introduction

The important properties of tin, such as malleability, ductility, and corrosion resistance, make it suitable for use in many applications [1–3]. Cassiterite is the main mineral for the cost-efficient extraction of tin. The Dachang ore field in the Guangxi province of China is one of the main sources of cassiterite associated with the sulfide ore; therefore, it is named cassiterite associated with pollimetallic ore (tin, lead, antimony, zinc, iron). Useful minerals of cassiterite associated with pollimetallic ore are cassiterite, pyrite, pyrrhotite, arsenopyrite, jamesonite, and small amounts of sphalerite, tetrahedrite tin, galena, and chalcopyrite, while gangue minerals are mainly quartz and calcite [4].

Cassiterite is heavy, hard, and extremely brittle; therefore, gravity separation was a frequently used method for recovering cassiterite [5,6]. On the other hand, sulfide minerals are generally recovered by flotation. Due to the different separation methods of cassiterite and sulfide minerals, the required grinding size is also different [4]. Coarsely ground ore, with particles larger than 40 µm, is required for recovering cassiterite [7]. If particles are smaller, the gravity separation efficiency sharply decreases. For recovering sulfide minerals, finely ground ore, with particles in the range of −0.15 + 0.010 mm, is necessary [4]. As present, in Chehe Dressing Plant in Guangxi, China, the cassiterite is recovered by shaking table, and the required particle size is about −0.148 + 0.40 mm. For recovery sulfide mineral, the required particle size is about 70% of −0.074 mm. However, it is challenging to meet both the requirements of rough grinding of cassiterite and fine grinding of sulfide. There is an inherent contradiction between cassiterite overgrinding and sulfide ore undergrinding.

The overgrinding would cause a large amount of cassiterite to be ground to a fine level, yielding a high loss rate in tailings, which is difficult to recover.

Some attempts were made to optimize the grinding size of cassiterite by rod mill [8], double-sphericity abnormity media [9], electric pulse fragmentation [10], thermal pretreatment [11], and grinding optimization (grinding media, grinding circuits and grinding models) [4,12–14]. To a certain extent, these above methods could improve the distribution of particle size in grinding product. Especially, thermal pretreatment can lead to thermal expansion of minerals, and then lead to intergranular cracking, and enhanced liberation. However, it needs a long time to heat the whole sample by traditional heating.

Therefore, microwave heating attracts a lot of attention. Microwave heating fundamentally differs from conventional heating because microwave electromagnetic energy can penetrate deep into the sample for an instant. Compared with traditional heating techniques, the main advantages of microwave heating in mineral processing are (i) non-contact heating, (ii) energy transfer instead of heat conduction and convection, (iii) rapid heating, (iv) selective heating, (v) volumetric heating, and (vi) heating from the interior of mineral body [15–17]. In the last few decades, microwave assisted grinding has been focused on ilmenite, chalcopyrite, iron ore, coal, gold ore, pyrite, and lead and zinc ore [18–24]. It is found that the grinding effect in microwave heating pretreatment is better than that in traditional heating. Compared to conventional processes, microwave leaching processes were found to be highly energy-efficient, less time consuming, and more environmentally friendly.

According to the plant process of Chehe Dressing Plant in Guangxi of China, the required particle size for recovering cassiterite by shaking table is about −0.148 + 0.40 mm, and the required particle size for recovering sulfide mineral by flotation is about 70% of −0.074 mm. In this paper, cassiterite associated with pollimetallic ore was subjected to microwave heating pretreatment in the hope that microwave selective heating of minerals could lead to selective thermal expansion and improve requirements of rough grinding of cassiterite and fine grinding of sulfide. Firstly, we assessed the ability of different minerals to absorb the microwave energy. Secondly, the influences of microwave heating and conventional heating pretreatment on grinding were carried out. The particle size, the grade of metal, and the metal distribution in each grinding product were analyzed before and after the heating pretreatment. Combined with the ability of mineral to absorb microwave, the influence of microwave selective heating on grinding was analyzed.

2. Materials, Equipment and Methods

2.1. Materials

Test samples (cassiterite associated with pollimetallic ore) were the jigging concentrate from Chehe Dressing Plant in Guangxi, China. The results of the semiquantitative analysis of the test sample are presented in Table 1. Ore minerals present in the test sample are mainly pyrite, jamesonite, sphalerite, and cassiterite, while gangue minerals are quartz, carbonate, and aluminosilicate minerals. The particle size distribution and the distribution of the main metal in each size of cassiterite associated with pollimetallic ore are shown in Tables 2 and 3, respectively. The metal element grade in each size is relatively homogeneous. The highest yield is for the particle size of −3 + 2 mm, in which most metals are distributed.

Table 1. The semiquantitative analysis results of the test sample (mass/%).

Composition	SiO_2	Fe_2O_3	SO_3	CaO	Al_2O_3	Zn	As	Sn	K_2O	MgO	Pb	P_2O_5	Sb	Mn	Other
Content/%	52.1	15.6	10.7	9.9	3.5	2.8	1.2	1.2	0.8	0.6	0.5	0.5	0.3	0.1	0.19

Table 2. The particle size distribution of cassiterite associated with pollimetallic ore.

Particle Size/mm	Yield/%	Cumulative Yield/%
−3.2 + 3	19.08	100.00
−3 + 2	43.12	80.92
−2 + 1	29.54	37.80
−1	8.26	8.26
Total	100.00	

Table 3. The analysis results of the main metal element in each size.

Range of Size/mm	Grade/%					Distribution Rate/%				
	Fe	Sn	Pb	Sb	Zn	Fe	Sn	Pb	Sb	Zn
−3.2 + 3	10.9	0.87	0.32	0.18	2.16	21.20	19.45	22.12	20.20	19.37
−3 + 2	10.04	0.85	0.3	0.19	2.1	44.12	42.94	46.86	48.19	42.57
−2 + 1	8.56	0.76	0.22	0.14	2.26	25.77	26.30	23.54	24.32	31.38
−1	10.6	1.17	0.25	0.15	1.72	8.922	11.32	7.48	7.29	6.68
Total						100	100	100	100	100

2.2. Equipment and Methods

A resistance furnace was used as traditional heating equipment (power is 12 kW). Figure 1 depicts a flow diagram of the microwave heating and grinding. The equipment mainly included a microwave oven, a resistance furnace, a conical ball mill (for wet grinding), a Bond power ball mill (for dry grinding), a vibration screen, an infrared imager, and a thermocouple thermometer. The output power of the microwave apparatus was 1–6 kW. It consisted of six air-cooled magnetrons operating at 2.45 GHz, a microwave cavity with a volume of about 80 L (power density is 1.25–7.5 $\times$ 10^4 W/m^{-3}), and a turntable to hold and rotate the sample vessel. A high purity quartz crucible was used as a sample container, and the cavity was filled with nitrogen when the experiment was performed. The temperatures for microwave heating and traditional heating were determined by decomposition temperature of minerals.

The ability of minerals to interact with microwaves determines the effect of microwave heating pretreatment on grinding. Therefore, the microwave absorption characteristics of jamesonite, pyrite, sphalerite, cassiterite, and gangue (quartz and calcite) were assessed through surface temperature (measured by TP80s infrared imaging, Figure S1, Supplementary Material), microwave heating curves (Figure S2). The microwave absorption ability was calorimetrically determined (Figure S3) [25–27], and magnetic and dielectric constants were obtained by a Network analyzer (N5244A PNA-X) (Figure S4) [28,29].

We used 500 g of cassiterite associated with pollimetallic ore for the microwave treatment. The microwave power was 6 kW. The sample was ground before and after the microwave pretreatment for 5 min by a ball mill (wet grinding) or 200r Bond ball index (dry grinding), respectively. Afterward, the sample was screened by the vibration screen. The metal element grade and the metal distribution in each particle size range were analyzed. Combined with the grinding test and ability of minerals in absorbing microwave, the grinding effect was discussed based on the content of metals and the distribution of metal elements.

The errors involved in the measurement and analysis of the result values were as follows: stability of microwave energy, mineral content and distribution in raw materials, and also ball mill. After a few repeat experiments, the errors involved in the measurement and analysis of the result values were small. It was acceptable.

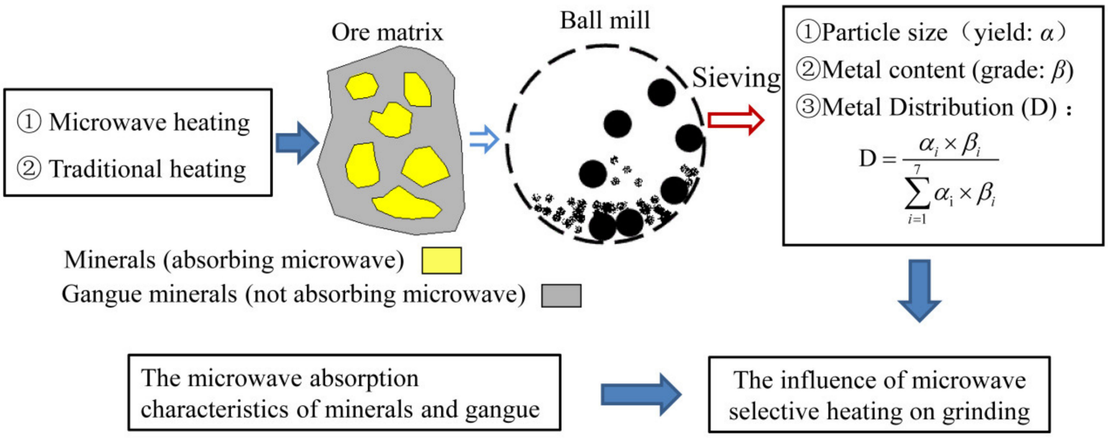

Figure 1. Flow diagram of the microwave heating and grinding.

3. The Microwave Absorption Ability of Minerals

The microwave absorption characteristics of jamesonite, pyrite, sphalerite, cassiterite, quartz, and calcite are presented in Figure 2a,b. The *RE* value (range of 0–100%) represents the relative microwave energy absorbed by the sample (see in the supporting information and Figure S4). The higher the *RE* value, the stronger the microwave absorption ability. The real permittivity of these six samples at 2.45 GHz is shown in Table 4.

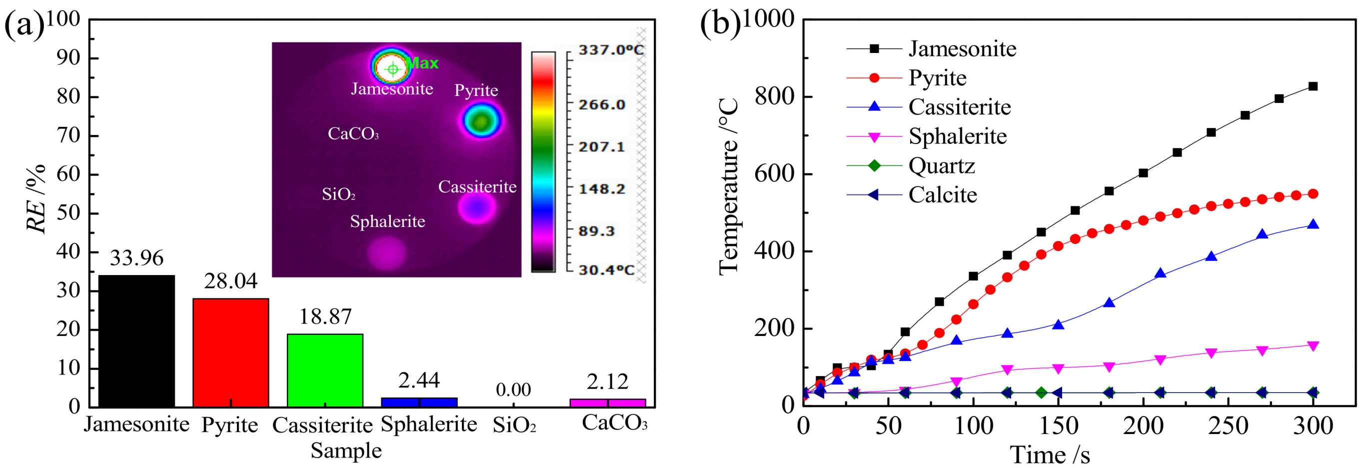

Figure 2. The ability of microwave absorption of minerals and gangues: (**a**) *RE* and (**b**) heating curve.

Table 4. Dielectric constants of the sample components at 2.45 GHz.

Sample	70% Sample + 30% Wax		
	ε′	ε″	tanδ
Jamesonite ($Pb_4FeSb_6S_{14}$)	6.7129	0.4498	0.0670
Pyrite (FeS_2)	8.1663	0.5473	0.0670
Cassiterite (SnO_2)	4.5484	0.2573	0.0566
Sphalerite (ZnS)	4.1924	0.0895	0.0213
Quartz	2.8034	0.0328	0.0117
Calcite	4.0132	0.0439	0.0109

Figure 2a shows significant differences in the microwave absorption ability of the main minerals in cassiterite associated with pollimetallic ore. Among them, jamesonite has the highest *RE* value, followed by pyrite, cassiterite, sphalerite, while gangue minerals are the worst. Besides, Figure 2a illustrates the surface temperature (measured by infrared imaging) of these six samples after being put together in a rotating table in the microwave heating field for 60 s (Figure S1). The surface temperature is consistent with the *RE* values, indicating that the higher *RE* is related to the stronger microwave absorption and the higher surface temperature. Figure 2b shows that microwaves easily heat jamesonite and pyrite. The heating rate of cassiterite is lower, while quartz and calcite are not significantly heated in the microwave field.

Table 4 shows that jamesonite, cassiterite, and pyrite exhibit good microwave absorption properties and can be heated by the microwave field through dielectric loss (Figure S5 and S6); in contrast, sphalerite, quartz, and calcite show weak microwave absorption, which is consistent with the data in Figure 2a. Therefore, based on the difference ability in absorbing microwave, microwave selective heating and selective thermal expansion can be achieved.

4. Grinding Test

4.1. Before and after the Microwave Pretreatment

The wet grinding test results of untreated samples, naturally cooled samples pretreated by microwave heating, and water-quenched samples pretreated by microwave (MW) heating are shown in Figure 3.

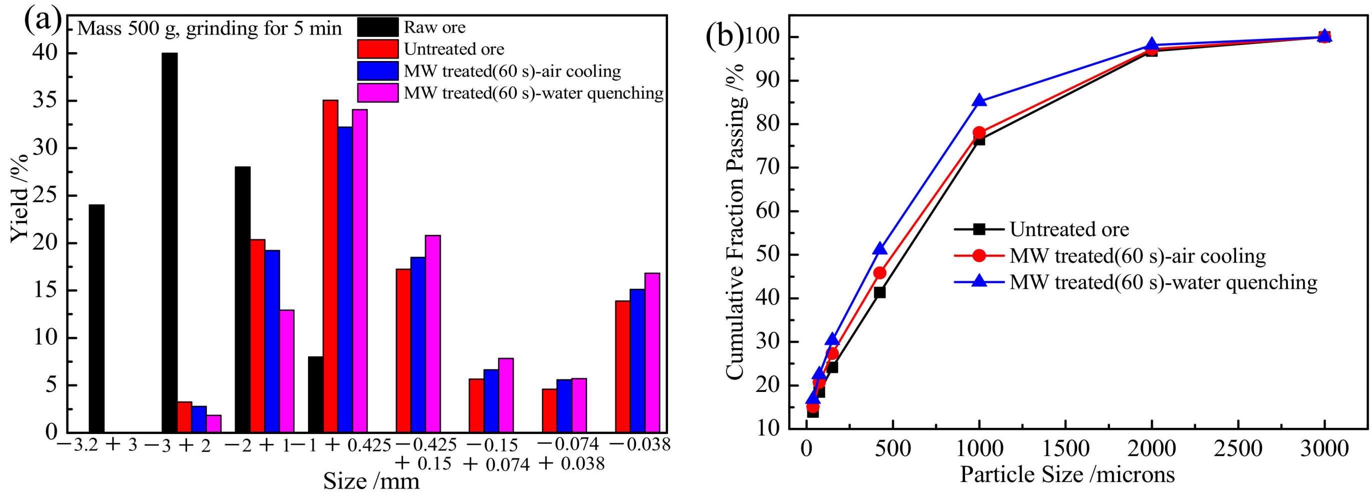

Figure 3. Effect of the cooling pattern on the particle size distribution after the microwave pretreatment: (**a**) yield and (**b**) cumulative fraction passing.

After the microwave heating for 60 s (the surface temperature seen in Figure S7), the surface temperature was about 340 °C. The yield of coarse particles (−2 + 1 mm) of the grinding products significantly decreases, while the yield of fine particles (−0.425 mm) increases. The changes in the particle size of grinding products are more apparent after water quenching. The microwave pretreatment with water quenching is more conducive to promoting the reduction of ore hardness, so that the increase in the yield of fine particles is more apparent.

The grade and distribution of Fe, Pb, Sn, and Zn in each particle size range are shown in Figure 4. The grade and distribution of Fe are significantly decreased in the size ranges of −3.2 + 2 mm, −2 + 1 mm, and −1 + 0.425 mm, and significantly increased in the size ranges of −0.15 + 0.074 mm, −0.15 + 0.074 mm, and −0.038 mm. Since pyrite exhibits good microwave absorption ability and represents a large fraction in the ore matrix. Pyrite was quickly heated in the microwave field, resulting in a thermal expansion and yielding the microcrack generation so that pyrite crushes first in the grinding process. The grinding rate and separation of pyrite are accelerated and promoted.

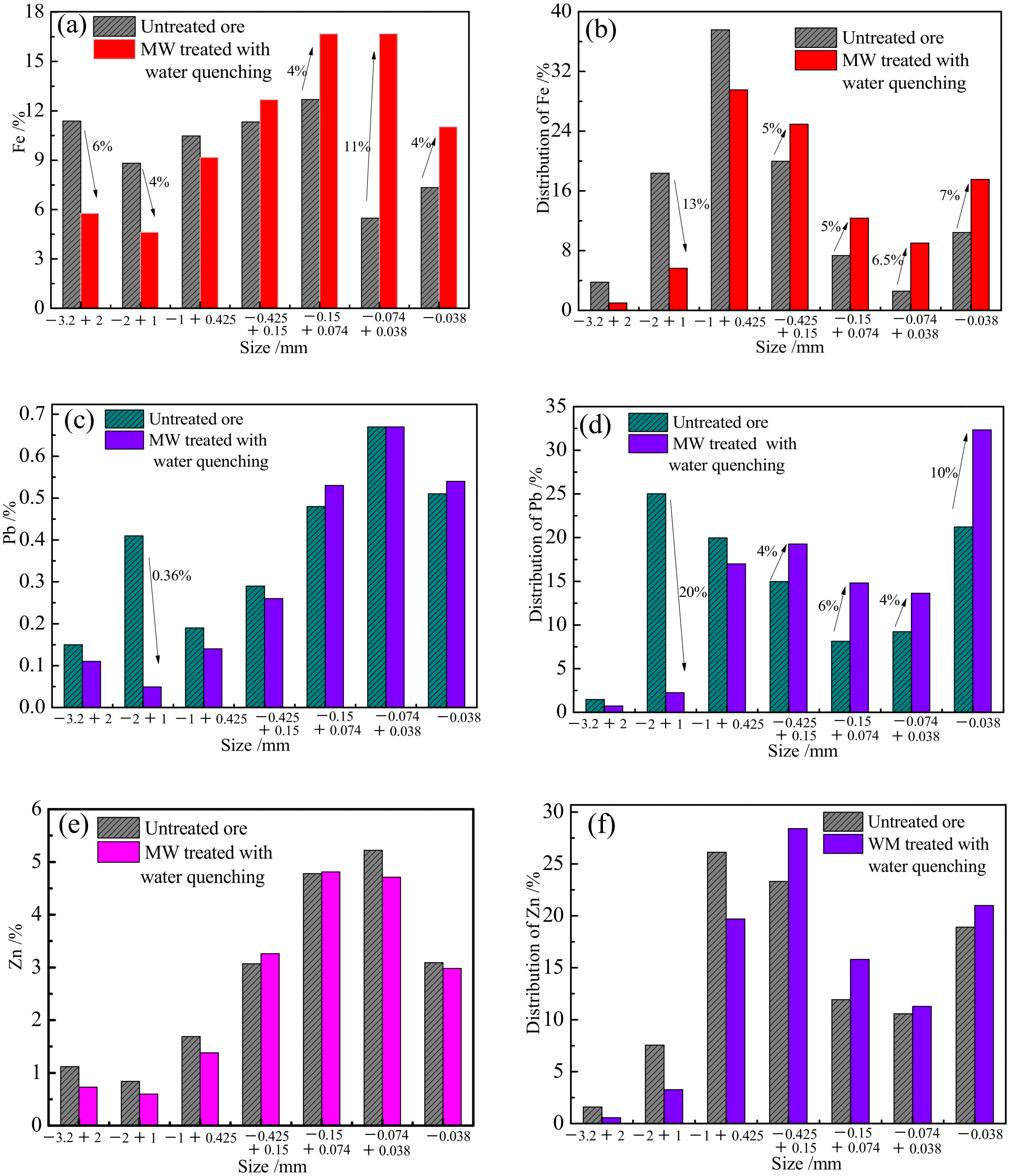

Figure 4. *Cont.*.

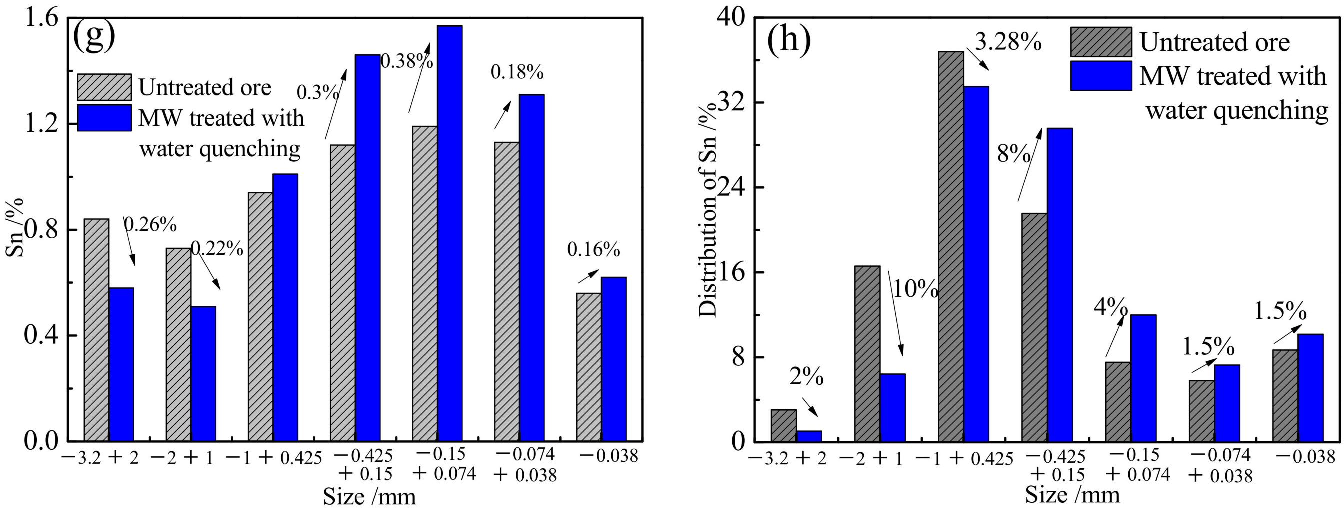

Figure 4. The grade and distribution of metal elements in each particle size range after grinding. (**a**) Fe grade, (**b**) Fe distribution, (**c**) Pb grade, (**d**) Pb distribution, (**e**) Zn grade, (**f**) Zn distribution, (**g**) Sn grade, and (**h**) Sn distribution.

The Pb grade and distribution in the coarse-size range of −2 + 1 mm decrease significantly, while the Pb grade changes slightly in the fine-size ranges of −0.15 + 0.074 mm, −0.15 + 0.074 mm, and −0.038 mm. However, the Pb distribution increases significantly in the size ranges of −0.15 + 0.074 mm, −0.074 + 0.038 mm, and −0.038 mm. Especially, the distribution in the size range of −0.038 mm increases considerably. This may originate from jamesonite's excellent microwave absorption ability, which can be heated up quickly in the microwave field. It yields thermal expansion and microcrack generation, increasing the grindability after the microwave pretreatment.

Sphalerite shows a weak microwave absorption ability, so it is not easy to heat in the microwave field. The grade and distribution of Zn before and after the microwave pretreatment change slightly, unlike Fe and Sn: it slightly decreases in the coarse-size range of 3 + 0.425 mm, while the Zn distribution in the size range of −0.425 mm increases little.

The grade and distribution of Sn decrease significantly in the sizes of −3.2 + 2 mm and −2 + 1 mm and increase in the size ranges of −0.425 + 0.15 mm and −0.15 + 0.074 mm, suggesting that the grindability of cassiterite is improved after the microwave heating pretreatment. This induces cassiterite priority crushing, but the effect is relatively weaker than for pyrite. The Sn distribution in the fine-size ranges of −0.074 + 0.038 mm and −0.038 mm increases by 1.5%. Therefore, the requirements of rough grinding of cassiterite and fine grinding of sulfide could be achieved by the microwave pretreatment.

4.2. Comparison of Microwave Heating and Traditional Heating

A resistance furnace was used as traditional heating equipment (power is 12 kW). The raw ore samples without any pretreatment (Untreated), microwave-heated (MW), and resistance furnace-heated (RFH) were dry ground by Bond power ball mill with 200 rotations. We set the sample grinding batch to 1000 g. After the dry grinding, the samples were screened.

4.2.1. The Temperature Influence in the Traditional Heating

After conventional heating for 20 min at different temperatures (based on decomposition temperature of minerals), the samples were immediately placed into water to cool down and dried for dry grinding and screening test, as shown in Table 5. The traditional heating pretreatment and microwave heating pretreatment improve the grinding effect (grindability). After the traditional heating pretreatment, the coarse particle size of the product gradually decreases with the heating temperature, while the fine particle size gradually increases, indicating that high temperatures are beneficial for grinding, which implies that temperature is the key factor for successful grinding.

Table 5. Effect of temperature in the traditional heating with water cooling on the particle size distribution of the grinding product.

Size/mm	Yield/%				
	Untreated	MW (1 min)	RFH (400 °C, 20 min)	RFH (500 °C, 20 min)	RFH (600 °C, 20 min)
−3.2 + 2	21.59	16.06	16.87	14.82	8.97
−2 + 1	24.26	21.79	21.66	20.98	21.71
−1 + 0.425	21.21	21.49	21.91	22.33	25.20
−0.425 + 0.15	14.96	18.04	17.62	18.34	19.36
−0.15 + 0.074	5.21	7.01	6.76	7.05	7.52
−0.074 + 0.038	3.32	5.11	4.72	5.26	5.67
−0.038	9.45	10.50	10.45	11.23	11.58
Total	100	100	100	100	100

4.2.2. The Influence of Heating Time in the Traditional Heating

Considering that the decomposition temperature of some sulfide minerals in the ore is around 495 °C (pyrite), the resistance furnace was set at 400 °C when studying the effect of the heating time in the traditional heating to avoid the influence of the arsenic and sulfur decomposition. The grinding test results are shown in Table 6.

Table 6. Effect of traditional heating time with water cooling on the particle size distribution of the grinding product.

Size/mm	Untreated	RFH				MW
		5 min	10 min	15 min	20 min	1 min
−3.2 + 2	21.59	21.32	20.45	18.57	16.87	16.06
−2 + 1	24.26	23.25	22.49	22.99	21.66	21.79
−1 + 0.425	21.21	19.47	20.01	20.18	21.91	21.49
−0.425 + 0.15	14.96	15.7	16.01	16.72	17.62	18.04
−0.15	17.98	20.26	21.03	21.54	21.93	22.62
Total	100	100	100	100	100	100

The coarse grain size gradually decreases with the heating time, while the fine grain size increases. The particle size distribution of the product after dry grinding through RFH at 400 °C for 20 min is similar to that after the application of the microwave field with a power 6 kW for 1 min (Figure S7). Compared with the pretreatment time of microwave heating (Table S1), the pretreatment time in traditional heating is considerably longer.

Tables 7–10 show the grade and distribution of Fe, Pb, Sn, and Zn for each size range of grinding products after traditional (12 kW, 20 min) and microwave heating pretreatments (6 kW, 1 min), respectively. Both heat treatments show that the Fe, Pb, and Zn grade and distribution in the coarse-size range (−3.2 + 2 mm, −2 + 1 mm) significantly decrease, while they increase in the size ranges of −0.425 + 0.15 mm, −0.15 + 0.074 mm, −0.074 + 0.038 mm, and −0.038 mm.

Table 7. Grade and distribution of Fe for each particle size range of the grinding product.

Size/mm	Fe %			Distribution of Fe/%		
	Untreated	MW (1 min)	RFH (20 min)	Untreated	MW (1 min)	RFH (20 min)
−3.2 + 2	12.22	6.76	8.29	22.24	9.41	11.74
−2 + 1	11.25	7.52	8.77	23.01	14.20	15.94
−1 + 0.425	11.44	10.98	11.62	20.45	20.45	21.37
−0.425 + 0.15	12.98	15.51	15.68	16.36	24.25	23.19
−0.15 + 0.074	14.70	19.90	19.18	6.45	12.10	10.88
−0.074 + 0.038	14.81	19.23	17.72	4.14	8.51	7.02
−0.038	9.23	12.17	11.25	7.35	11.08	9.86
Total				100.00	100.00	100.00

Table 8. Grade and distribution of Pb for each particle size range of the grinding product.

Size/mm	Pb %			Distribution of Pb/%		
	Untreated	MW (1 min)	RFH (20 min)	Untreated	MW (1 min)	RFH (20 min)
−3.2 + 2	0.26	0.06	0.15	17.29	3.31	7.65
−2 + 1	0.21	0.10	0.13	15.69	7.29	8.51
−1 + 0.425	0.26	0.18	0.25	16.98	13.07	16.56
−0.425 + 0.15	0.38	0.42	0.43	17.51	25.60	22.91
−0.15 + 0.074	0.56	0.65	0.64	8.98	15.41	13.09
−0.074 + 0.038	0.71	0.73	0.73	7.25	12.60	10.43
−0.038	0.56	0.64	0.66	16.29	22.72	20.84
Total				100.00	100.00	100.00

Table 9. Grade and distribution of Zn for each particle size range of the grinding product.

Size/mm	Zn %			Distribution of Zn/%		
	Untreated	MW (1 min)	RFH (20 min)	Untreated	MW (1 min)	RFH (20 min)
−3.2 + 2	1.32	0.72	0.78	11.77	4.66	5.30
−2 + 1	1.07	0.71	0.85	10.72	6.23	7.41
−1 + 0.425	2.09	1.81	1.93	18.31	15.66	17.03
−0.425 + 0.15	3.90	4.12	3.99	24.09	29.92	28.31
−0.15 + 0.074	5.72	5.50	5.50	12.31	15.53	14.98
−0.074 + 0.038	6.28	5.64	5.67	8.60	11.59	10.78
−0.038	3.64	3.88	3.85	14.20	16.41	16.19
Total				100.00	100.00	100.00

Table 10. Grade and distribution of Sn for each particle size range of the grinding product.

Size/mm	Sn %			Distribution of Sn/%		
	Untreated	MW (1 min)	RFH (20 min)	Untreated	MW (1 min)	RFH (20 min)
−3.2 + 2	1.14	0.64	0.62	24.96	10.10	9.71
−2 + 1	0.87	0.67	0.71	21.41	14.35	14.27
−1 + 0.425	1.11	1.10	1.27	23.87	23.22	25.82
−0.425 + 0.15	0.92	1.48	1.53	13.96	26.23	25.02
−0.15 + 0.074	1.04	1.63	1.67	5.49	11.24	10.48
−0.074 + 0.038	1.24	1.44	1.50	4.17	7.22	6.57
−0.038	0.64	0.74	0.84	6.13	7.64	8.14
Total				100.00	100.00	100.00

However, there are also differences between traditional and microwave heating. The Fe, Pb, and Zn grade and metal distribution in the coarse-size range after the microwave heating are lower than after the traditional heating. In the fine-size range, the grade and metal distribution of Fe and Pb after the microwave heating are higher than after the traditional heating, indicating the selective microwave heating for pyrite and jamesonite, and the microwave heating time is shorter than the traditional heating time. Additionally, crushing occurs first for the minerals that absorb microwaves, which is the main difference between the microwave and traditional heating pretreatments.

The grade and distribution of Sn (Table 10), similar to Section 4.1 (wet grinding), decreases significantly in the size ranges of −3.2 + 2 mm and −2 + 1 mm, and increases in the size ranges of −0.425 + 0.15 mm and −0.15 + 0.074 mm. Still, the fraction of Sn slightly increases in the size range of −0.038 mm. The distributions of Fe, Pb, and Zn in fine-size range are higher than Sn, indicating that it can promote the separation of sulfide ore and reduce cassiterite overgrinding by controlling grinding parameters and heating treatment.

4.2.3. Energy Consumption

In order to compare the energy consumption of the traditional and microwave heating pretreatments, the energy consumption of the heating pretreatments with a similar grinding effect was analyzed and shown in Table 11.

Table 11. Comparison of the electric energy consumption of the two heating pretreatments.

Heating Equipment	Sample Mass/g	Power/kW	Time/min	Energy Consumption/kJ	Energy Processing 1 t of Ore/kJ
Resistance furnace	1000	12	20	14.4×10^3	14.4×10^6
Microwave oven	500	6	1	3.6×10^2	7.2×10^5

According to a rough calculation, the energy consumption of the microwave heating treatment is only 5% of that of the traditional heating pretreatment. The energy consumption of the resistance furnace does not consider the energy consumption for the heating from room temperature to 400 °C (1.5 h). Thus, the energy consumption in the traditional heating pretreatment greatly exceeds the microwave energy consumption. In the traditional heating, the whole ore sample is heated from the surface toward the inside, taking a long time, while microwaves selectively heat specific minerals in the ore matrix but not other gangue minerals. In addition, the higher the microwave power density, the shorter the time required [18,19].

5. Conclusions

Cassiterite polymetallic sulfide was pretreated by traditional and microwave heating pretreatments. Jamesonite and pyrite exhibited good microwave absorption, and they could be quickly heated to high temperatures in the microwave field. Both heat pretreatments improved the grinding effect, especially for the coarse-size range (−3.2 + 2 mm, −2 + 1 mm). The distribution of Fe, Pb, Zn, and Sn increased in the fine-size range (−0.425 mm). The selective microwave heating of pyrite and jamesonite played a key role. The Fe and Pb grades in the size ranges of −3.2 + 2 mm and −2 + 1 mm after the microwave pretreatment (6 kW, 1 min) were lower than those after the traditional heating (12 kW, 400 °C, 20 min). The grade and distribution of Sn decreased significantly in the size ranges of −3.2 + 2 mm and −2 + 1 mm, and increased in the size ranges of −0.425 + 0.15 mm and −0.15 + 0.074 mm. The fraction of Sn slightly increased in the size range of -0.038 mm. Heating treatment promoted the liberation of sulfide ore and reduced cassiterite overgrinding. The microwave heating time was shorter than the traditional heating time. The minerals that exhibited a stronger microwave absorption ability crushed first. The energy consumption of the microwave heating pretreatment was only 5% of that consumed in the traditional heating pretreatment.

Supplementary Materials: The following are available online at https://www.mdpi.com/article/10.3390/min11070768/s1. Figure S1. Schematic illustration of multiple materials discretely coexisted. 1. Magnetron, 2. Waveguide, 3. Turntable, 4. Microwave cavity, Figure S2. Microwave apparatus for heating curves. 1. Magnetron, 2. Antenna cap, 3. Waveguide, 4. Thermal insulation, 5. Sample, 6. Quartz crucible, 7. Thermocouple, 8. Metal shielding tube, 9. Digital thermometer, 10. Microwave cavity, 11. Turntable. Figure S3. Diagram of measuring apparatus. 1. Test materials, 2. Quartz container, 3. Metal cabinet, 4. Microwave oven, 5. Plastic box, 6. Water medium, 7. Operation panel, 8. Ceramic plate, 9. Microwave outlet of waveguide, 10. Thermal insulation material (quartz fiber), Figure S4. The scheme of magnetic and dielectric properties measurement. 1. Computer, 2. Network analyzer, 3. Coaxial transmission line, 4. Sample, 5. Outer conductor, 6. Inner conductor, Figure S5. Dielectric properties of the sulphide ore and SnO_2: (a) ε', (b) ε'', (c) $\tan\delta$, Figure S6. Dielectric properties of calcite and quartz (a) ε', (b) ε'', (c) $\tan\delta$, Figure S7. Effect of microwave heating time on distribution of surface temperature of test sample, Table S1. Effect of microwave heating time with water cooling on size distribution of grinding product (6 kW, 500 g).

Author Contributions: Conceptualization, C.H. and X.S.; methodology, C.H. and X.S.; validation, Y.W. and T.F.; investigation, C.H., J.Y. and Z.W.; resources, S.M.; data curation, J.Z.; writing—original draft preparation, C.H.; writing—review and editing, Y.W. and T.F.; supervision, T.F.; project administration, S.M.; funding acquisition, C.H. All authors have read and agreed to the published version of the manuscript.

Funding: This research was funded by Natural Science Foundation of China, grant number 51804084, Science and Technology Major Project of Guangxi Province, grant number AA18118030, and Natural Science Foundation Guangxi Province, grant number 2018GXNSFAA281337.

Data Availability Statement: The raw/processed data required to reproduce these findings cannot be shared at this time as the data also forms part of an ongoing study.

Acknowledgments: We want to acknowledge the support of Chehe Dressing plant in Guangxi, China and Kaituo Wang for his advice.

Conflicts of Interest: The authors declare no conflict of interest.

References

1. Xu, G.L.; Zhang, L.; He, C.Z.; Ma, D.W.; Lu, Z.S. Adsorption and oxidation of NO on various SnO_2(110) surfaces: A density functional theory study. *Sensor. Actuat. B Chem* **2015**, *221*, 717–722. [CrossRef]
2. Soliś-Casados, D.; Vigueras-Santiago, E.; Hernández-López, S.; Camacho-López, M.A. Characterization and photocatalytic performance of tin oxide. *Ind. Eng. Chem. Res* **2009**, *48*, 1249–1252. [CrossRef]
3. Bakr, Z.H.; Wali, Q.; Yang, S.; Yousefsadeh, M.; Padmasree, K.P.; Ismail, J.; Ab Rahim, M.H.; Yusoff, M.M.; Jose, R. Characteristics of ZnO- SnO_2 composite nanofibers as a photoanode in dye-sensitized solar cells. *Ind. Eng. Chem. Res* **2019**, *58*, 643–653. [CrossRef]
4. Yang, J.; Shuai, Z.; Zhou, W.; Ma, S. Grinding Optimization of Cassiterite-Polymetallic Sulfide Ore. *Minerals* **2019**, *9*, 134. [CrossRef]
5. Angadi, S.I.; Sreenivas, T.; Jeon, H.-S.; Baek, S.-H.; Mishra, B.K. A review of cassiterite beneficiation fundamentals and plant practices. *Miner. Eng.* **2015**, *70*, 178–200. [CrossRef]
6. Feng, Q.C.; Zhao, W.J.; Wen, S.M.; Cao, Q.B. Activation mechanism of lead ions in cassiterite flotation with salicylhydroxamic acid as collector. *Sep. Purif. Technol* **2017**, *178*, 193–199. [CrossRef]
7. Lu, Y.X.; Wang, S.; Zhong, H. Optimization of conventional hydroxamic acid for cassiterite flotation: Application of structural modification under principle of isomerism. *Miner. Eng.* **2021**, *167*, 106901. [CrossRef]
8. Xue, T.L.; Guangxi University. Study on Selective Grinding Behavior for Cassiterite Polymetallic Sulfide Ore. 2014. Available online: http://cdmd.cnki.com.cn/Article/CDMD-10593-1014370271.htm (accessed on 13 July 2021).
9. Mo, W.; Feng, J.P.; Ma, S.J.; Yang, J.L.; Su, X.J. Study on Grinding by a Double-Sphericity Abnormity Media. *Appl. Mech. Mater.* **2013**, *333–335*, 2010–2014. [CrossRef]
10. Brua, K.; Sousa, R.; Leite, M.M.; Broadbent, C.; Stuart, G.; Pashkevich, D.; Martin, M.; Kern, M.; Parvaz, D.B. Pilot-scale investigation of two Electric Pulse Fragmentation (EPF)approaches for the mineral processing of a low-grade cassiterite schist ore. *Miner. Eng.* **2020**, *150*, 106270. [CrossRef]
11. Wills, B.A.; Parker, R.H.; Binns, D.G. Thermally assisted liberation of cassiterite. *Min. Metall. Explor.* **1987**, *4*, 94–96. [CrossRef]
12. Yang, J.L.; Zhou, W.T.; MA, S.J.; Yang, X.J.; Mo, F. Study on cassiterite polymetallic sulfide ore grinding optimization based on the grinding technical efficiency. *Nonferrous Met. Miner. Process. Sect.* **2017**, *5*, 18–22. Available online: http://en.cnki.com.cn/Article_en/CJFDTotal-YSXK201705005.htm (accessed on 13 July 2021).
13. Zhou, W.T.; Han, Y.X.; Li, Y.J.; Yang, J.L.; Ma, S.J.; Sun, Y.S. Research on prediction model of ore grinding particle size distribution. *J. Dispers. Sci. Technol.* **2020**, *41*, 537–546. [CrossRef]
14. Ma, S.J.; Mo, W.; Wang, G.F.; Su, X.J.; Shi, Z.W. Study on ball mill grinding of a cassiterite polymetallic sulfide ore. In Proceedings of the International Mineral Processing Congress (IMPC 2010), Brisbane, Australia, 6–10 September 2010; pp. 991–999.
15. Pickles, C.A. Microwaves in extractive metallurgy: Part 1-Review of fundamentals. *Miner. Eng.* **2009**, *22*, 1102–1111. [CrossRef]
16. Haque, K.E. Microwave energy for mineral treatment processes-a brief review. *Int. J. Miner. Process.* **1999**, *57*, 1–24. [CrossRef]
17. Walkiewicz, J.W.; Kazonich, G.; McGill, S.L. Microwave heating characteristics of selected minerals and components. *Miner. Metall. Process.* **1988**, *5*, 39–42. [CrossRef]
18. Vorster, W.; Rowson, N.A.; Kingman, S.W. The effect of microwave radiation upon the processing of Neves Corvo copper ore. *Int. J. Miner. Process.* **2001**, *63*, 29–44. [CrossRef]
19. Whittles, D.N.; Kingman, S.W.; Reddish, D.J. Application of numerical modelling for prediction of the influence of power density on microwave-assisted breakage. *Int. J. Miner. Process.* **2003**, *68*, 71–91. [CrossRef]
20. Jones, D.A.; Kingman, S.W.; Whittles, D.N.; Lowndes, I.S. Understanding microwave assisted breakage. *Miner. Eng.* **2005**, *18*, 659–669. [CrossRef]
21. Kingman, S.W.; Jackson, K.; Bradshaw, S.M.; Rowson, N.A.; Greenwood, R. An investigation into the influence of microwave treatment on mineral ore comminution. *Powder Technol.* **2004**, *146*, 176–184. [CrossRef]
22. Omran, M.; Fabritius, T.; Abdel-Khalek, N.; El-Aref, M.; Elmanawi, A.E.-H.; Nasr, M.; Elmahdy, A. Microwave assisted liberation of high phosphorus oolitic iron ore. *J. Miner. Mater. Charact. Eng.* **2014**, *2*, 414–427. [CrossRef]
23. Omran, M.; Fabritius, T.; Mattila, R. Thermally assisted liberation of high phosphorus oolitic iron ore: A comparison between microwave and conventional furnaces. *Powder Technol.* **2015**, *269*, 7–14. [CrossRef]

24. Amankwah, R.K.; Ofori-Sarpong, G. Microwave heating of gold ores for enhanced grindability and cyanide amenability. *Miner. Eng.* **2011**, *24*, 541–544. [CrossRef]
25. He, C.L.; Ma, S.J.; Su, X.J.; Chen, Y.Q.; Liang, Y.S. Calorimetry study of microwave absorption of some solid materials. *J. Microw. Power Electromagn. Energy* **2013**, *47*, 251–261. [CrossRef] [PubMed]
26. He, C.L.; Ma, S.J.; Su, X.J.; Mo, Q.H.; Yang, J.L. Comparison of the microwave absorption characteristics of hematite, magnetite and pyrite. *J. Microw. Power Electromagn. Energy* **2015**, *49*, 131–146. [CrossRef]
27. Ma, S.J.; Zhou, X.W.; Su, X.J.; Mo, W.; Yang, J.L.; Liu, P. A new practical method to determine the microwave energy absorption ability of materials. *Miner. Eng.* **2009**, *22*, 1154–1159. [CrossRef]
28. Song, N.N.; Ke, Y.J.; Yang, H.T.; Zhang, H.; Zhang, X.Q.; Shen, B.G.; Cheng, Z.H. Integrating giant microwave absorption with magnetic refrigeration in one multifunctional intermetallic compound of $LaFe_{11.6}Si_{1.4}C_{0.2}H_{1.7}$. *Sci. Rep.* **2013**, *3*, 2291. [CrossRef]
29. Hotta, M.; Hayashi, M.; Nagata, K. High temperature measurement of complex permittivity and permeability of Fe_3O_4 powders in the frequency range of 0.2 to 13.5 GHz. *ISIJ Int.* **2011**, *51*, 491–497. [CrossRef]